# Extraction of the chemical contribution to the interfacial magnetic anisotropy in Ni/$Cu_3Au$(001)

Na Lei,[1,*] Liu Yang,[1] Dahai Wei,[2] Yuan Tian,[3] and Xiaofeng Jin[3,†]

[1]*Fert Beijing Institute, MIIT Key Laboratory of Spintronics, School of Integrated Circuit Science and Engineering, Beihang University, Beijing 100191, China*

[2]*State Key Laboratory of Superlattices and Microstructures, Institute of Semiconductors, Chinese Academy of Sciences, Beijing 100083, China*

[3]*State Key Laboratory of Surface Physics and Department of Physics, Fudan University, Shanghai 200433, China*

(Received 29 September 2021; revised 2 December 2021; accepted 16 December 2021; published 3 January 2022)

The manipulation of magnetic anisotropy via interface is crucial for spintronics, but its mechanism is still controversial due to the parasitic problem of strain and the chemistry environment. We have independently controlled the interfacial chemistry of the epitaxially grown Ni film on $Cu_3Au$(001) by inserting the thickness wedged Cu layer. The Ni layer is confirmed to be fully strained until 8 ML by the analysis of LEED I-V spectra, which guarantees that the strain contributions to the magnetic anisotropies are identical. Our results clearly show that the chemistry contribution of Au atoms at Ni/$Cu_3Au$ interface plays a major role for its perpendicular magnetic anisotropy. We provide a method to quantitatively separate and extract the chemistry and strain contributions to the interfacial magnetic anisotropy, which is helpful for clarifying its mechanism and developing high performance spintronic materials and devices.

DOI: 10.1103/PhysRevB.105.024402

## I. INTRODUCTION

The control of magnetic anisotropy in ultrathin films has emerged as a topic of importance, especially to achieve the perpendicular magnetic anisotropy (PMA) [1–7]. This is not only of fundamental interest but also important for industrial applications, such as high-density magnetic recording, magnetic random access memory, and other potential spintronic devices [3,4,8–11]. The interface is getting crucial to determine their magnetic properties [12,13] when the films are getting into ultrathin scale, like MgO/CoFeB thin film, which is one of the most promising material systems in spintronic devices [14–20]. Modifying the interfacial chemistry surroundings in MgO/CoFeB/nonmagnetic metals (NMs: Ta, W, Mo etc.) heterostructure is a common method to enhance the interfacial PMA. However, due to the lattice mismatches between CoFeB and NMs, the strain contribution for the interfacial PMA must be taken into account. The mixed contributions from the chemistry and strain of the NMs hinder the clairification of the intrinsic mechanisms in the strong PMA. Up to now, it lacks a well-defined way to distinguish and separate these two contributions experimentally. Here, we developed a method to extract the chemistry effect on the interfacial magnetic anisotropy with strain kept the same in a representative Ni/$Cu_3Au$(001) system.

The pseudomorphically grown Ni film on Cu(001) is a prototype to explore the various contributions to magnetic anisotropies, which has been intensively studied [21–31]. The Ni films exhibit perpendicular magnetization for a thickness from 10.5 to around 70 ML where spin orientation transitions (SRTs) occur. Its PMA is mainly from the bulk magnetoelastic anisotropy contribution, countering the interfacial anisotropy and demagnetization. Since the strain in Ni films plays an important role in the emergence of PMA, one may expect to achieve stronger PMA by lattice expansion [32,33]. A very recent work realized a high perpendicular magnetic anisotropy in Ni/Pt superlattices [7], and proved that the strain effect is the prime source. Nevertheless, with in-plane lattice constant changing from 0.352 to 0.372 nm, besides the bulk anisotropy strongly enhanced, the interfacial anisotropy also increased considerably. Therefore, to clarify the origin of magnetic anisotropy, one needs to tune the chemistry and strain, and check their contributions independently. Here, we choose $Cu_3Au$(001), whose lattice constant is 0.373 nm, as a substrate to study the chemistry effect on the interfacial anisotropy.

In Ni/$Cu_3Au$(001), the Ni films exhibit perpendicular magnetization between 5 and 12 ML [33], which is consistent with the expectation of larger bulk anisotropy ($K_b$) in Ni films compared to the Ni/Cu(001) system. However, there is a well-known Au segregation on $Cu_3Au$(001) surface. The $c(2 \times 2)$ reconstruction indicates an Au rich surface with 50% of Au atoms [34]. The chemical Au contribution for the interfacial anisotropy has so far been ignored when comparing the magnetic anisotropies of Ni films on Cu(001) and $Cu_3Au$(001). Here, we covered the $Cu_3Au$(001) surface with a Cu wedge layer and effectively tune the interface layer from $Cu_3Au$ to pure Cu continuously. Meanwhile, all the ultrathin epitaxial layers are fully strained with their lateral lattice constants same as that of $Cu_3Au$(001). We observed the perpendicular anisotropy of Ni films vanishes with increasing Cu coverage layer up to 1 ML.

## II. EXPERIMENTS AND RESULTS

All experiments were carried out in an ultrahigh vacuum system with the pressure lower than $3 \times 10^{-10}$ mbar during

*To whom correspondence should be addressed: na.lei@buaa.edu.cn

†xfjin@fudan.edu.cn

 

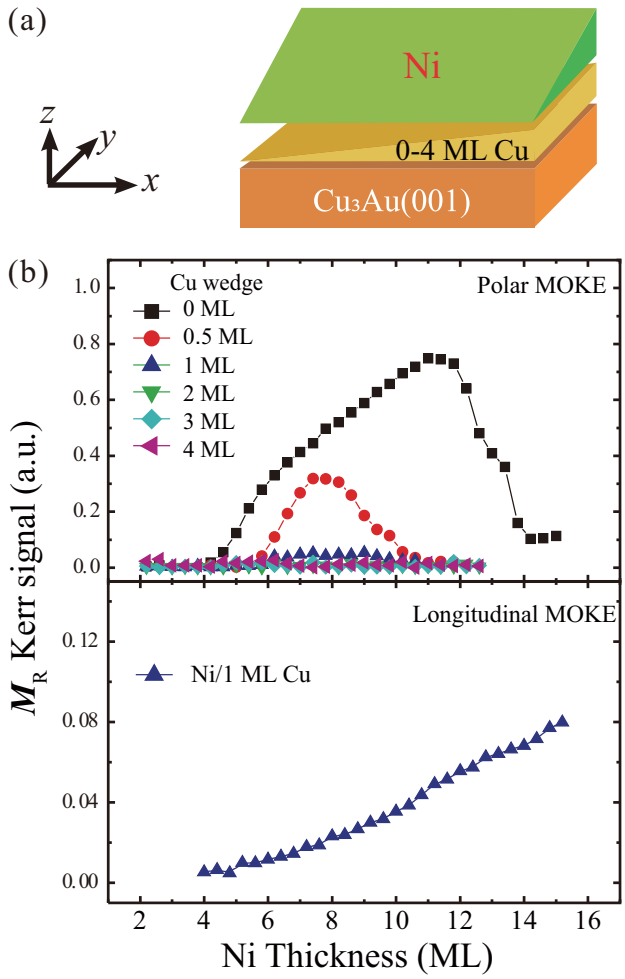


FIG. 1. (a) Schematic structure of the double wedged 2–15 ML Ni/0–4 ML $Cu/Cu_3Au(001)$. (b) Remnant polar (top panel) and longitudinal (bottom panel) Kerr ellipticity of Ni on 0–4 ML $Cu/Cu_3Au(001)$ and 1 ML $Cu/Cu_3Au(001)$, respectively. All MOKE measurements were performed at 220 K.

the deposition. $Cu_3Au(001)$ substrate was thoroughly cleaned by $Ar^+$ bombardment, followed by annealing at 850 K for 10 min, and then kept at 620 K for 20 min. This cleaning procedure was repeated until a sharp $c(2 \times 2)$ low energy electron diffraction (LEED) pattern was observed with a large amount of atomically flat terraces seen by scanning tunneling microscope (STM). Ni, Au, and Cu metal pieces with a purity of 99.99% were used as the evaporating sources. The deposition rates were predetermined by a quartz microbalance before evaporation, while the accurate thickness of the deposited layers was further calibrated by the coverage of atomic terraces in STM images [13]. The perpendicular and in-plane magnetizations were characterized *in situ* at a low temperature of 223 K by magneto-optical Kerr effect (MOKE) with polar and longitudinal modes, respectively. The lattice relaxation of Ni and Cu films in $z$ axis was checked by kinematic LEED I-V spectra measurements at room temperature.

The schematic structure of the double wedged 2–15 ML Ni/0–4 ML $Cu/Cu_3Au(001)$ sample is shown in Fig. 1(a), with the thicknesses of Cu and Ni layers varying along $x$ and $y$ directions, respectively. Cu thickness wedge from 0 to 4 ML was covered on $Cu_3Au(001)$ substrate to isolate the influence from the Au atoms at the interface. After the growth of Ni films on 0–4 ML $Cu/Cu_3Au(001)$, the hysteresis loops are measured by MOKE at 223 K immediately. The remnant magnetization $M_R$ is extracted from the loops, as shown in Fig. 1(b). The remnant polar Kerr ellipticity is shown in the top panel, and the out-of-plane signal from 5 to 12 ML is observed for $Ni/Cu_3Au(001)$ (solid black square), which is consistent with previous study [12]. However, it decreases dramatically as Cu layer is capped on $Cu_3Au(001)$. For 0.5 ML Cu, a much smaller out-of-plane signal (solid red dots) can be seen in the thickness range of about 6–9 ML. No out-of-plane signal can be observed when Cu layer is more than 1 ML. Longitudinal MOKE was also performed to further verify the magnetization orientation, as shown by the bottom panel in Fig. 1(b). It confirms the in-plane remnant magnetization when 1 ML Cu is capped on $Cu_3Au(001)$.

The surface of 0–4 ML Cu covered on $Cu_3Au(001)$ was characterized by LEED ($E = 70$ eV), as shown in Figs. 2(a)–2(c). For the bare $Cu_3Au(001)$ substrate, the sharp $c(2 \times 2)$ reconstruction is observed, which is attributed to the Au segregation on the surface [34]. The line profiles taken along the white dashed lines are plotted on its right side, the peaks for $(-1/2, -1/2)$ spot can be clearly seen at the center. These Au atoms at the surface can be effectively covered by a few monolayers of Cu capped at room temperature. With increasing the thickness of Cu layer, the (1/2, 1/2) spot vanishes gradually and the peak intensity in the line profile decreases, shown in Figs. 2(b) and 2(c). A clear and sharp $(1 \times 1)$ LEED pattern is achieved for 4 ML $Cu/Cu_3Au(001)$, since the LEED is surface sensitive with a small probe depth of few nm at low energy region. Additionally, we can conclude that the epitaxially grown Cu layers follow the lateral lattice constant of $Cu_3Au(001)$ since the line-profile peak positions of $(-1, 0)$ and $(0, -1)$ spots do not shift from top to bottom.

Moreover, the vertical lattice constant $a_\perp$ of the Cu capping layer was studied by the kinematic analyses of LEED I-V spectra, as shown in Figs. 2(d) and 2(e). The intensity of (0, 0) spot was recorded as a function of the incident electron beam energy. The black and red spectra are of Cu(001) and $Cu_3Au(001)$ substrate as references, and the blue spectra are of 1–4 ML Cu on $Cu_3Au(001)$, respectively. All spectra have offset for clarity. According to the Bragg's law, diffraction peak appears when $n\lambda = a_\perp \sin\theta$, where $\lambda$ is the wavelength of incident electron beam, $\theta$ is the incident angle of electron beams, which is set to 89.5 deg for convenience of recording the (0, 0) spot. Energy peaks appear at $E_{00}^n = \frac{1.504}{a_\perp^2} n^2$. The dashed vertical lines in Fig. 2(d) correspond to the $n = 6^{\text{th}}$ diffraction peaks of $Cu_3Au(001)$, Cu(001) substrate and Cu capping layers on $Cu_3Au(001)$, respectively.

The peak positions $E_{00}^n$ for Cu(001), $Cu_3Au(001)$ and 4ML $Cu/Cu_3Au(001)$ are marked by the black arrows in Fig. 2(d) and plotted versus $n^2$ in Fig. 2(e). The linear relation between $E_{00}^n$ and $n^2$ can be clearly seen and the vertical lattice constants are extracted from the linear fitting. We obtained $a_\perp$ of Cu(001), $Cu_3Au(001)$ and Cu layer on top are 0.361 $\pm$ 0.002 nm, 0.3725 $\pm$ 0.002 nm and 0.341 $\pm$ 0.001 nm, respectively. According to elastic theory, the associated vertical (compressive) stress $\varepsilon_2 = -\frac{2c_{12}}{c_{11}}\varepsilon_1$, where $c_{11}$ and $c_{12}$ are the cubic elastic stiffness constants. For the fully strained

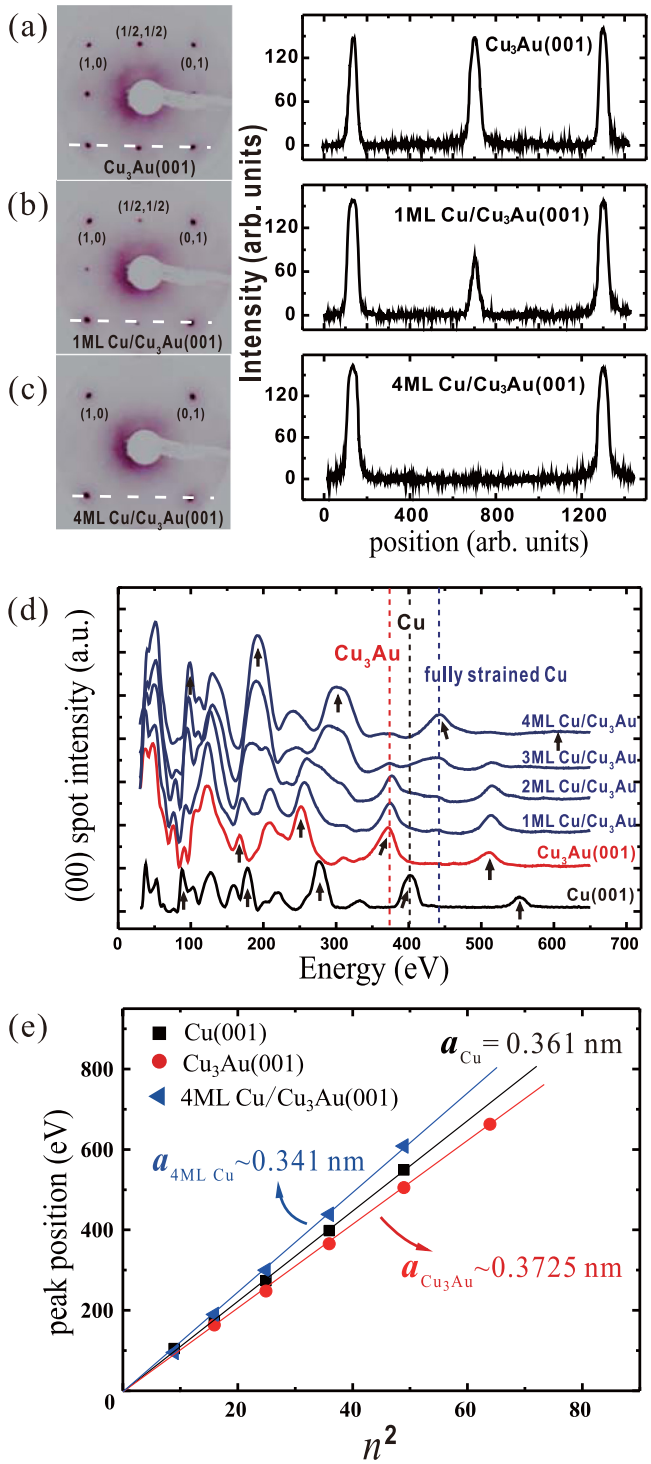


FIG. 2. (a)–(c) LEED patterns of bare $Cu_3Au(001)$ substrate, 1 ML Cu and 4 ML Cu on $Cu_3Au(001)$ are taken at $E = 70$ eV; the correspondence line profiles are shown on the right. (d) (0, 0) spot kinematic LEED I-V spectra of Cu(001), $Cu_3Au(001)$ and 0–4 ML Cu layers capped on $Cu_3Au(001)$. Arrows indicate the position of elastic diffraction peaks, and vertical dashed lines mark peaks with $n = 6$. (e) The peak positions $E_n$ are plotted versus $n^2$ for Cu(001), $Cu_3Au(001)$ and 0–4 ML Cu layers capped on it. The vertical lattice constants are extracted from the linear fitting, respectively.

Cu films grown on $Cu_3Au(001)$, the lateral (tensile) stress is $\varepsilon_1 = 3.3\%$. Taking into account the stiffness constants of Cu [35], we can get $\varepsilon_2 = -4.8\%$, thus the vertical lattice constant of Cu film on $Cu_3Au(001)$ is estimated to be 0.344 nm, which is consistent with the value extracted from LEED I-V. We can conclude that the Cu layers are fully strained with their lateral lattice constants following $Cu_3Au(001)$ substrate up to 4 ML.

In order to further confirm that the out-of-plane magnetization in Ni films is induced by the Au atoms at interface, a well-defined sample structure is prepared via shadow mask deposition as shown in Fig. 3(a), which contains three different areas: (I) $Ni/Cu_3Au(001)$; (II) Ni/1 ML $Cu/Cu_3Au(001)$; (III) Ni/0.5 ML Au/1 ML $Cu/Cu_3Au(001)$, with the interfaces of Ni-$Cu_3Au$, Ni-Cu and Ni-CuAu, respectively.

For clarification the in-plane magnetization with 1 ML Cu insertion, the strain in Ni films on 1 ML $Cu/Cu_3Au(001)$ is studied and compared with that on $Cu_3Au(001)$. The LEED I-V spectra are shown in Fig. 3(b), the black and red lines are the spectra of 3, 5, 8, and 12 ML Ni films on areas (I) and (II) from bottom to top, respectively. The dashed vertical lines are used to mark the 5th and 6th diffraction peaks. For both spectra, the peaks slightly shift to lower energy as the Ni film thickness increased, indicating the strain relaxed gradually in the Ni films. Nevertheless, no relative peak shift can be distinguished between the two black and red spectra for the same Ni thicknesses. We can conclude that the insertion of 1 ML Cu between Ni and $Cu_3Au(001)$ substrate does not change the strain in the Ni films, i.e., $\Delta\varepsilon_2 < 0.5\%$, the upper limit of the uncertainty. The bulk anisotropy $K_b$ in Ni films should be identical with $Ni/Cu_3Au(001)$. Therefore, the magnetization orientation difference between $Ni/Cu_3Au(001)$ and Ni/1 ML $Cu/Cu_3Au(001)$ in Fig. 1(b) could be only from the different interface chemistry condition (Cu and CuAu), where the Ni/CuAu interface prefers out-of-plane magnetization compared with the one of Ni/Cu.

The polar MOKE results in these three areas are shown in Fig. 3(c). For the top panel, the out-of-plane magnetization between 5 and 12 ML is shown in $Ni/Cu_3Au(001)$. For the middle panel, as 1 ML Cu is inserted, no out-of-plane magnetization can be observed. Surprisingly, the out-of-plane magnetized Ni films show up again when 0.5 ML Au deposited on the 1 ML Cu to forming a CuAu surface [similar with $Cu_3Au(001)$], as shown in the bottom panel. This experiment unambiguously shows that the perpendicular magnetization of 5–12 ML Ni films on $Cu_3Au(001)$ is induced by Au atoms at the interface. The results in area (I) and (III) show slight difference, which is presumably due to roughness and defects induced by the 0.5 ML Au/1 ML Cu, as compared to the $Cu_3Au(001)$.

## III. DISCUSSION

The interfacial magnetic anisotropy energy of thin films is estimated quantitively based on the phenomenological formula [28]:

$$K = (K_s + K_i)/d + K_b - E_d, \quad (1)$$

where $K_b$ is the bulk anisotropy, $K_s$ and $K_i$ are the interfacial anisotropies for the upper and bottom interfaces, and $E_d$ is

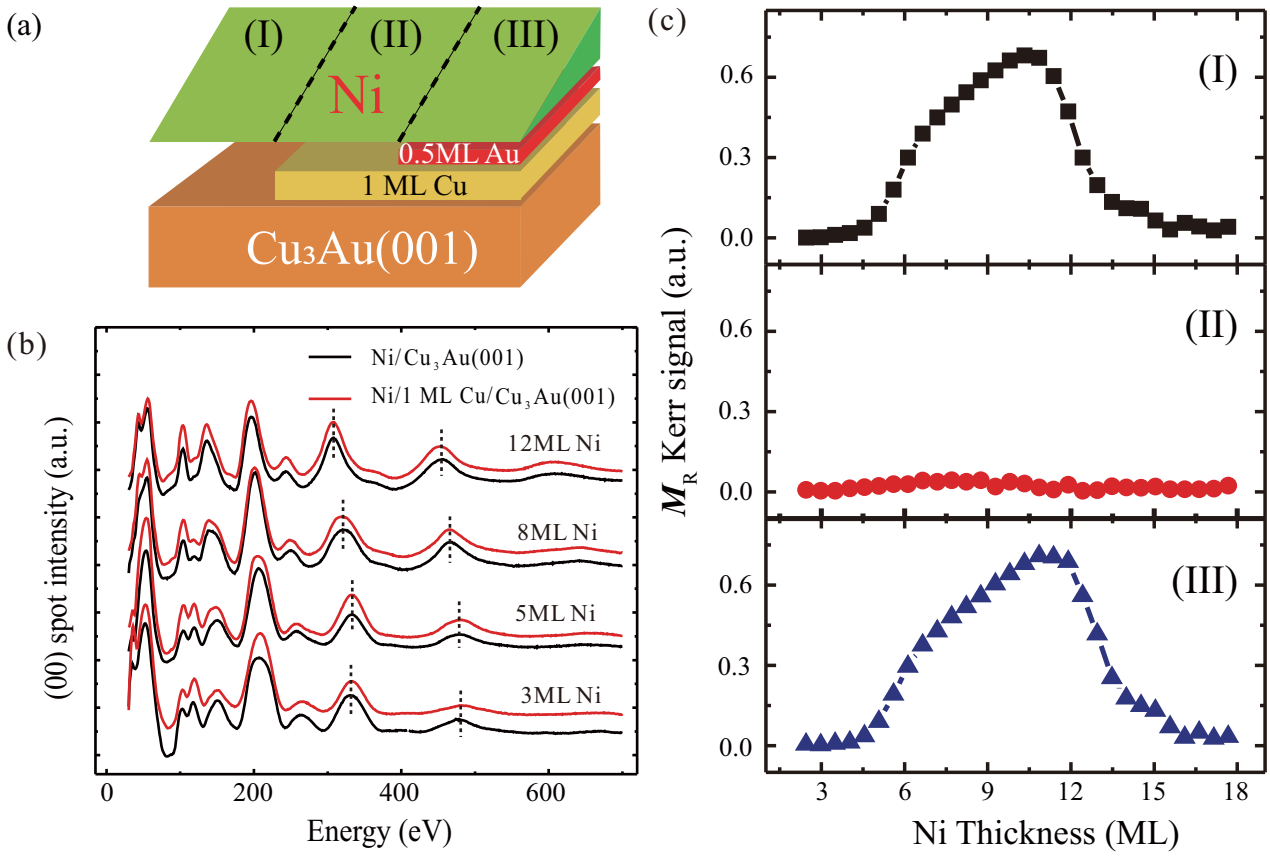


FIG. 3. (a) Structure scheme of sample. (b) LEED I-V spectra are 3, 5, 8, and 12 ML Ni films on $Cu_3Au(001)$ (black solid line) and 1 ML $Cu/Cu_3Au(001)$ (red solid line) respectively. (c) Polar Kerr ellipticity of area (I) $Ni/Cu_3Au(001)$, area (II) Ni/1 ML $Cu/Cu_3Au(001)$, and area (III) Ni/0.5 ML Au/1 ML $Cu/Cu_3Au(001)$, measured at 223 K.

the demagnetization energy. The $K_b$ due to the magnetoelastic effect, are 30 $\mu$eV/atom [29] and 70.4 $\mu$eV/atom [33] for Ni films on Cu(001) and $Cu_3Au(001)$, respectively. They are not related to the condition of interface, but only proportional to the film strain $\varepsilon_1$. The demagnetization energy $E_d$ is constant for Ni films as 7.5 $\mu$eV/atom [29]. The critical thickness $d_c$ of the magnetization orientation switching from in-plane to out-of-plane (1st SRT) can be written as

$$d_c = -(K_s + K_i)/(K_b - E_d). \quad (2)$$

In Ni/Cu(001), $K_b^{Cu} = 30\,\mu$eV/atom, $E_d = 7.5\,\mu$eV/atom, $d_c = 10.5$ ML [29]. While for $Ni/Cu_3Au(001)$, the Ni film is fully strained ($\varepsilon_1 = 5.9\%$) below 8 ML as shown by the LEED-IV results in Fig. 3(b), and its bulk anisotropy energy is estimated to be $K_b^{Cu3Au} = 70.4\,\mu$eV/atom. The $d_c$ for $Ni/Cu_3Au(001)$ with a $Cu_3Au$ interface is determined to be 5 ML, while it shifts to 6 ML for Ni/0.5 ML $Cu/Cu_3Au(001)$ with half monolayer Cu inserted, as shown by the black squares and red dots in Fig. 1(b), respectively.

Here we chose the system of Ni films on $x$ ML $Cu/Cu_3Au(001)$ for analysis, where less than 1 ML Cu is considered ($0 \leqslant x \leqslant 1$). The bulk magnetic anisotropies $K_b$ and the upper interfacial anisotropies $K_s$ are kept the same regardless of the ultrathin Cu inserting layer [as indicated in Fig. 3(b)]. While the bottom interfacial terms $K_i$ are significantly tuned since the Cu layer changes the interfacial conditions of the bottom interface. According to the STM morphologies, the ultrathin Cu layers are epitaxially grown on $Cu_3Au(001)$ with atomic terraces, as shown in the Supplemental Material Fig. S1 [36]. The Ni film on $x$ ML $Cu/Cu_3Au(001)$ can be simply considered as two parts: Ni on the 1 ML Cu atomic terrace (with an area ratio of $x$) and Ni on the bare $Cu_3Au(001)$ surface (with an area ratio of $1–x$). Thus, the total bottom interfacial magnetic anisotropy $K_i$ can be written as

$$K_i = xK_i^{Cu} + (1-x)\,K_i^{Cu3Au}, \quad (3)$$

where $K_i^{Cu}$ and $K_i^{Cu3Au}$ are the interfacial anisotropies for Ni-Cu and $Ni-Cu_3Au$ interfaces on the $Cu_3Au(001)$ substrate, respectively. Then

$$d_c^x = -\left[K_s + xK_i^{Cu} + (1-x)K_i^{Cu3Au}\right]/\left(K_b^{Cu3Au} - E_d\right). \quad (4)$$

As for Ni/1 ML $Cu/Cu_3Au(001)$, no SRT can be observed and the $K_i$ cannot be directly estimated according to Eq. (4). Here we take the result of $x = 0.5$, where $d_c^{0.5} = 6$ ML, as shown in Fig. 1(b). Then the total interfacial anisotropy energies of Ni/Cu and $Ni/Cu_3Au$ can be extracted as: $K_s + K_i^{Cu} = -440.3\,\mu$eV/atom and $K_s + K_i^{Cu3Au} = -314.5\,\mu$eV/atom, with the lateral lattice constant of 0.373 nm. The difference of the bottom interfacial anisotropy energies $\Delta K_i$ can be obtained: $K_i^{Cu} - K_i^{Cu3Au} = -125.8\,\mu$eV/atom, indicating the chemistry contribution of Cu atoms at the interface prefers in-plane magnetization. The strain, interface and magnetic

TABLE I. Comparison of magnetic anisotropies of Ni on 0–1 ML $Cu/Cu_3Au(001)$ and Cu(001).

| | $Ni/Cu_3Au(001)$ | Ni/0.5 ML $Cu/Cu_3Au(001)$ | $Ni/Cu/Cu_3Au(001)$ | Ni/Cu(001)[Ref. 26] |
|---|---|---|---|---|
| *Strain* | 5.9% | 5.9% | 5.9% | 2.5% |
| $K_b$ | 70.4 $\mu$eV/atom | 70.4 $\mu$eV/atom | 70.4 $\mu$eV/atom | 30 $\mu$eV/atom |
| *Bottom interface* | Ni-$Cu_3Au$ | 50%Ni-$Cu_3Au$ + 50%Ni-Cu | Ni-Cu | Ni-Cu |
| $d_c$ | 5 ML | 6 ML | N.A. | 10.5 ML |
| $K_s + K_i$ | −314.5 $\mu$eV/atom | −377.4 $\mu$eV/atom | −440.3 $\mu$eV/atom | −236.2 $\mu$eV/atom |

anisotropies of Ni films on $x$ ML $Cu/Cu_3Au(001)$ ($x = 0$, 0.5 and 1) and Cu(001) have been summarized in the Table I. We can conclude that the Ni/Au interface anisotropy energy is much lower than Ni/Cu.

## IV. CONCLUSION

In summary, the magnetic anisotropy of Ni films on $Cu_3Au(001)$ is studied with changing the interface from $Cu_3Au$ to pure Cu under the same lateral lattice constant. With increasing the Cu coverage at the interface, the perpendicular magnetic anisotropy of Ni films decreases dramatically and switches to in-plane when Cu thickness is higher than 1 ML. Compared to the Ni/Cu interface, Au atoms at the interface significantly affects the interfacial anisotropy, which induces the perpendicular anisotropy in Ni films from 5 to 12 ML on $Cu_3Au(001)$ substrate. This work clearly demonstrated that the interfacial magnetic anisotropy can be changed up to 125.8 $\mu$eV/atom with the interfacial chemical conditions, clarifies the previous interpretation of strain induced the change of SRT in $Ni/Cu_3Au(001)$ compared to Ni/Cu(001) system. Our research paves an alternative method to give an insight view of the interfacial magnetic anisotropy, which is crucial for the future manipulation of magnetic anisotropies.

## ACKNOWLEDGMENTS

This work was supported by the National Natural Science Foundation of China (Grants No. 12074025, No. 52061135105, No. 11774339, and No. 11421404), and the National Basic Research Program of China (Grant No. 2016YFA0300703).

[1] S. Mangin, D. Ravelosona, J. A. Katine, M. J. Carey, B. D. Terris, and E. E. Fullerton, Nat. Mater. **5**, 210 (2006).
[2] S. Ikeda, K. Miura, H. Yamamoto, K. Mizunuma, H. D. Gan, M. Endo, S. Kanai, J. Hayakawa, F. Matsukura, and H. Ohno, Nat. Mater. **9**, 721 (2010).
[3] A. D. Kent and D. C. Worledge, Nat. Nanotechnol. **10**, 187 (2015).
[4] S. S. P. Parkin and S.-H. Yang, Nat. Nanotechnol. **10**, 195 (2015).
[5] H. Cheng, J. Chen, S. Peng, B. Zhang, Z. Wang, D. Zhu, K. Shi, S. Eimer, X. Wang, Z. Guo, Y. Xu, D. Xiong, K. Cao, and W. Zhao, Adv. Electron. Mater. **6**, 2000271 (2020).
[6] X. Zhao, S. Mao, H. Wang, D. Wei, and J. Zhao, Appl. Phys. Lett. **118**, 092401 (2021).
[7] T. Seki, M. Tsujikawa, K. Ito, K. Uchida, H. Kurebayashi, M. Shirai, and K. Takanashi, Phys. Rev. Mater. **4**, 064413 (2020).
[8] I. M. Miron, K. Garello, G. Gaudin, P. J. Zermatten, M. V. Costache, S. Auffret, S. Bandiera, B. Rodmacq, A. Schuhl, and P. Gambardella, Nature (London) **476**, 189 (2011).
[9] Y. Xu, D. Chen, S. Tong, H. Chen, X. Qiu, D. Wei, and J. Zhao, Phys. Rev. Appl. **14**, 034064 (2020).
[10] T. Lin, H. Liu, S. Poellath, Y. Zhang, B. Ji, N. Lei, J. J. Yun, L. Xi, D. Z. Yang, T. Xing, Z. L. Wang, L. Sun, Y. Z. Wu, L. F. Yin, W. B. Wang, J. Shen, J. Zweck, C. H. Back, Y. G. Zhang, and W. S. Zhao, Phys. Rev. B **98**, 174425 (2018).
[11] W. Li, L. Bykova, S. Zhang, G. Yu, R. Tomasello, M. Carpentieri, Y. Liu, Y. Guang, J. Gräfe, M. Weigand, D. M. Burn, G. V. D. Laan, T. Hesjedal, Z. Yan, J. Feng, C. Wan, J. Wei, X. Wang, X. Zhang, H. Xu, C. Guo, H. Wei, G. Finoccio, X. Han, and G. Schütz, Adv. Mater. **31**, 1807683 (2019).
[12] F. Hellman, A. Hoffmann, Y. Tserkovnyak, G. S. D. Beach, E. E. Fullerton, C. Leighton *et al.*, Rev. Mod. Phys. **89**, 025006 (2017).
[13] N. Lei, D. H. Wei, C. S. Tian, S. H. Xiao, D. Z. Hou, L. H. Zhou, and X. F. Jin, Appl. Phys. Lett. **95**, 192506 (2009).
[14] A. Soumyanarayanan, N. Reyren, A. Fert, and C. Panagopoulos, Nature (London) **539**, 509 (2016).
[15] S. Peng, W. Zhao, J. Qiao, L. Su, J. Zhou, H. Yang, Q. Zhang, Y. Zhang, C. Grezes, P. Amiri, and K. Wang, Appl. Phys. Lett. **110**, 072403 (2017).
[16] T. C. Chuang, C. F. Pai, and S. Y. Huang, Phys. Rev. Appl. **11**, 061005(R) (2019).
[17] D. C. Worledge, G. Hu, D. W. Abraham, J. Z. Sun, P. L. Trouilloud, J. Nowak, S. Brown, M. C. Gaidis, E. J. O'Sullivan, and R. P. Robertazzi, Appl. Phys. Lett. **98**, 022501 (2011).
[18] G. Yu, Z. Wang, M. Abolfath-Beygi, C. He, X. Li, K. L. Wong, P. Nordeen, H. Wu, G. P. Carman, X. Han, I. A. Alhomoudi, P. K. Amiri, and K. L. Wang, Appl. Phys. Lett. **106**, 072402 (2015).
[19] B. Fang, X. Zhang, B. Zhang, Z. Zeng, and J. W. Cai, AIP Adv. **5**, 067116 (2015).
[20] X. Li, G. Yu, H. Wu, P. Ong, K. Wong, Q. Hu, F. Ebrahimi, P. Upadhyaya, M. Akyol, N. Kioussis, X. Han, P. K. Amiri, and K. L. Wang, Appl. Phys. Lett. **107**, 142403 (2015).
[21] R. Allenspach and A. Bischof, Phys. Rev. Lett. **69**, 3385 (1992).
[22] J. Thomassen, F. May, B. Feldmann, M. Wuttig, and H. Ibach, Phys. Rev. Lett. **69**, 3831 (1992).
[23] Z. Q. Qiu, J. Pearson, and S. D. Bader, Phys. Rev. Lett. **70**, 1006 (1993).
[24] R. Allenspach, M. Stampanoni, and A. Bischof, Phys. Rev. Lett. **65**, 3344 (1990).

[25] C. Chappert, K. L. Dang, P. Beauvillain, H. Hurdequint, and D. Renard, Phys. Rev. B **34**, 3192 (1986).
[26] R. Vollmer, Th. Gutjahr-Löser, J. Kirschner, S. van Dijken, and B. Poelsema, Phys. Rev. B **60**, 6277 (1999).
[27] W. L. O'Brien and B. P. Tonner, Phys. Rev. B **49**, 15370 (1994).
[28] B. Schulz and K. Baberschke, Phys. Rev. B **50**, 13467 (1994).
[29] S. van Dijken, R. Vollmer, B. Poelsema, and J. Kirschner, J. Magn. Magn. Mater. **210**, 316 (2000).
[30] J. Hong, R. Q. Wu, J. Lindner, E. Kosubek, and K. Baberschke, Phys. Rev. Lett. **92**, 147202 (2004).
[31] D. Sander, W. Pan, S. Ouazi, and J. Kirschner, W. Meyer, M. Krause, S. Müller, L. Hammer, and K. Heinz, Phys. Rev. Lett. **93**, 247203 (2004).
[32] W. C. Lin, B. Y. Wang, Y. W. Liao, Ker-Jar Song, and Minn-Tsong Lin, Phys. Rev. B **71**, 184413 (2005).
[33] A. Braun, B. Feldmann, and M. Wuttig, J. Magn. Magn. Mater. **171**, 16 (1997).
[34] Yasuo Fujinaga, Surf. Sci. **86**, 581 (1979).
[35] Y. F. Gao and Z. Suo, J. Mech. Phys. Solids **51**, 147 (2003).
[36] See Supplemental Material at http://link.aps.org/supplemental/10.1103/PhysRevB.105.024402 for STM morphologies of Cu on $Cu_3Au(001)$.